

Approximate Well Width and Optical Gain Formulas of 1.55 μm $\text{In}_{1-x-y}\text{Ga}_y\text{Al}_x\text{As}$ Compressively Strained Quantum-Well Laser*

ZHANG Ye-jin, CHEN Wei-you, JIANG Heng, LIU Cai-xia and LIU Shi-yong

(State Key Laboratory on Integrated Optoelectronics, Jilin University Region, Changchun 130023, China)

Abstract: Using Harrison's model and anisotropic parabolic approximation, the band structure of $\text{In}_{1-x-y}\text{Ga}_y\text{Al}_x\text{As}$ compressively strained quantum wells is calculated. To design lasers with 1.55 μm wavelength, it is necessary to analyze the well width, differential gain, transparency carrier density and the characteristic gain for an arbitrary composition. Some useful empirical formulas are also presented.

Key words: $\text{In}_{1-x-y}\text{Ga}_y\text{Al}_x\text{As}$; QW; linear gain; differential gain

PACC: 4255P; 4260; 7340L; 7280

CLC number: TN248.4

Document code: A

Article ID: 0253-4177(2001)01-0011-07

1 Introduction

It is well known that there are two main material systems used to fabricate long-wavelength semiconductor lasers, $\text{In}_{1-x}\text{Ga}_x\text{As}_{1-y}\text{P}_y$ system and $\text{In}_{1-x-y}\text{Ga}_y\text{Al}_x\text{As}$ system. The former has been studied extensively^[1,2], but the latter is applied only recently and with some high quality results yielded^[3-5]. For an $\text{In}_{1-x-y}\text{Ga}_y\text{Al}_x\text{As}$ system, large band offset $\Delta E_c/\Delta E_g$, from 0.47 eV to 0.7 eV, presents better electron confinement, which can improve the temperature stability.

In the device design, the threshold current, $L-I$ characteristics and modulation speed of a quantum-well laser can be optimized by varying the material compositions or strain. Some useful parameters can facilitate the design of certain emission wavelength lasers, such as well width, differential gain, trans-

parency carrier density and characteristic gain. In $\text{In}_{1-x}\text{Ga}_x\text{As}_{1-y}\text{P}_y$ system, some results^[6] given by Ma prove helpful for the design of 1.55 μm quantum-well lasers. For $\text{In}_{1-x-y}\text{Ga}_y\text{Al}_x\text{As}$ system, Minch presented the relations between composition, strain and bandgap, but without any further application in the device design^[5]. In this paper, the relations between well width, transparency carrier density, characteristics gain, differential gain and the material compositions are introduced. Some empirical formulas are also presented for the purpose of further applications.

Using Harrison's model, the band offset is obtained, which has less errors than that from the model-solid theory^[5]. Considering the nonparabolic band structure, we find that results from the anisotropic parabolic band expression are in good agreement with those from the experiment^[7].

* Project Supported by National Natural Science Foundation of China Under Grant No. 69937019, Jilin Province's Science Fund for Youth No. 19990529-2 and by National Research and Development Plan for High Technology of China (863 Plan) No. 863-307-15-3(08).

ZHANG Ye-jin was born in Jilin Province, China, in November 1973. He received the B.S. degree of semiconductor physics and device from Jilin University, Changchun, in 1996. Then, he joined National Integrated Optoelectronics Laboratories. He is now a Ph.D student at Jilin University. He has been engaged in research work on CAD for laser device.

Received 6 July 2000, revised manuscript received 17 September 2000

©2001 The Chinese Institute of Electronics

2 Theory

2.1 Calculation of Band Offset

With Chuang's approach, we calculate the band offset of $\text{In}_{1-x-y}\text{Ga}_y\text{Al}_x\text{As}$ system^[5]. To obtain some parameters of $\text{In}_{1-x-y}\text{Ga}_y\text{Al}_x\text{As}$ material system, a linear interpolation is applied between the parameters of relevant binary semiconductors. The interpolation formula is given as Eq. (1)^[8], with all physical parameters P except for the bandgap being used in the calculation of the band

edge.

$$P_{(\text{In}_{1-x-y}\text{Ga}_y\text{Al}_x\text{As})} = (1-x-y)P_{(\text{InAs})} + yP_{(\text{GaAs})} + xP_{(\text{AlAs})} \quad (1)$$

The material parameters of binary semiconductors can be found in Table 1. One exception to the linear interpolation is the formulas for the unstrained bandgap. In the $\text{In}_{1-x-y}\text{Ga}_y\text{Al}_x\text{As}$ system, the quality is given as^[5]

$$E_g(x, y) = 0.36 + 2.093x + 0.629y + 0.577x^2 + 0.436y^2 + 1.013xy - 2.0xy(1-x-y) \text{ eV} \quad (2)$$

Table 1 Parameters Used in the Calculation

Parameter	Symbol/unit	GaAs	InAs	AlAs	Ref.
Electron Effective Mass	m_e/m_0	0.067	0.023	0.15	[8]
Valence Band Parameter	γ_1	6.8	20.4	3.45	[8]
	γ_2	1.9	8.3	0.68	[8]
	γ_3	2.73	9.1	1.29	[8]
Hydrostatic Deformation Potential					
For Conduction Band	a_c/eV	-7.17	-5.08	-5.64	[5]
For Valence Band	a_v/eV	1.16	1.00	2.47	[5]
Shear Deformation Potential	b/eV	-1.7	-1.8	-1.5	[5]
Lattice Constant	a/nm	0.56533	0.60584	0.5660	[8]
Elastic Stiffness Constant	$C_{11}/(10^{11}\text{dyn} \cdot \text{cm}^2)$	11.879	8.329	12.5	[5]
Elastic Stiffness Constant	$C_{12}/(10^{11}\text{dyn} \cdot \text{cm}^2)$	5.376	4.526	5.34	[5]
Conduction Band Position	E_c^H/eV	1.53	0.801	2.525	[5]
Valence Band Position	E_v^H/eV	0.111	0.441	-0.425	[5]

In Harrison's model, the positions of the conduction and valence bands are determined by

$$E_c(x, y) = E_c^H + \delta E_c(x, y) \quad (3)$$

$$E_v(x, y) = E_v^H + \max(\delta E_{hh}(x, y), \delta E_{lh}(x, y)) \quad (4)$$

where $E_v^H(x, y)$ and $E_c^H(x, y)$ are obtained by a linear interpolation of binary parameters listed in Table 1; and δE_{hh} , δE_{lh} and δE_c are the unstrained energy shift as follows:

$$\delta E_c = 2a_c(1 - \frac{C_{12}}{C_{11}})\epsilon, (001) \quad (5)$$

$$\delta E_{hh} = 2a_v(1 - \frac{C_{12}}{C_{11}})\epsilon + b(1 + 2\frac{C_{12}}{C_{11}})\epsilon, (001) \quad (6)$$

$$\delta E_{lh} = 2a_v(1 - \frac{C_{12}}{C_{11}})\epsilon - b(1 + 2\frac{C_{12}}{C_{11}})\epsilon, (001) \quad (7)$$

where a_c and a_v are the conduction and valence band

hydrostatic deformation potential, and b is the valence band shear deformation potential. $\epsilon = (a_0 - a)/a$ is the strain in the plane of the epitaxial growth. a is the lattice constant of the quaternary epitaxial layer, while a_0 is that of the substrate.

The band-offset then can be calculated by

$$\frac{\Delta E_c}{\Delta E_g} = \frac{E_c^b - E_c^w}{(E_v^w - E_v^b) + (E_c^b - E_c^w)} \quad (\text{compressive strain}) \quad (8)$$

where the superscripts w and b indicate the well and barrier materials, respectively.

Figure 1 shows the relations between the band offset and Al composition with different Ga composition. In Harrison's model, band offsets calculated are close to the experimental ones^[5], ranging from 0.47eV to 0.7eV.

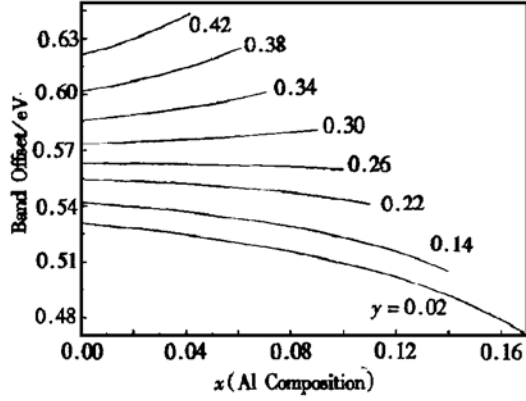


FIG. 1 Band Offset for $\text{In}_{1-x-y}\text{Ga}_y\text{Al}_x\text{As}$ System with Typical 1.25Q Barrier Lattice Matched to InP

2.2 Calculation of Band Structure and Gain

A simplified analytical band structure of strained quantum-well has recently been developed using an efficient decoupling method, with which the original 4×4 valence band Hamiltonian can be transformed into two blocks of 2×2 upper and lower Hamiltonians. As a result of decoupling, an analytical expression can be derived^[9].

$$-E = \frac{\eta^2 r_1}{2m_0} (k_x^2 + k_z^2) \pm \left[\left(\frac{\eta^2 r_2}{2m_0} (k_x^2 - 2k_y^2) + \zeta \right)^2 + 3 \left(\frac{\eta^2 r_2}{2m_0} k_x^2 \right)^2 + 12 \left(\frac{\eta^2 r_3}{2m_0} \right)^2 k_x^2 k_z^2 \right]^{1/2} \quad (9)$$

$$\zeta = -b \left(1 + 2 \frac{C_{12}}{C_{11}} \right) \epsilon$$

The strain is notated as ζ and the compressive strain is represented as negative ζ . To convert the non-parabolic bulk band structure above into a suitable form, we fit the valence band to the following anisotropic band expression^[9], with a large range covering all the optical transitions in k -space.

$$-E = \frac{\eta^2 k_x^2}{2m_{vx}m_0} + \frac{\eta^2 k_z^2}{2m_{vz}m_0} \quad (10)$$

Once the band structure is simplified to an anisotropic parabolic form, we can use the conventional approaches to analyze the carrier density and the optical transition probabilities. The effective mass perpendicular to the plane (m_{vz}) determines the quantum subband levels (or quantum confinement effects) and the optical transition energies.

Both the (2-D) density and joint density of the states of each subband depend on the effective mass in the plane (m_{vx}).

The local gain due to the transition from level j in the conduction band to level i in the valence band is^[9],

$$g_{ij}(E_{ij}^0) = \left(\frac{2\pi}{\eta} \right) |H_{ij}|^2 (f_j' - f_i') \left(\frac{\epsilon_1}{nc} \right) \rho_{ij}^x$$

$$\rho_{ij}^x = \rho_{ij}^{x0} h(\eta\omega - E_{ij}^0)$$

$$|H_{ij}|^2 = \left(\frac{q}{m_0} \right)^2 \left(\frac{2\eta\omega}{4\epsilon_1\epsilon_0\omega^2} \right) M_{ij}^2 \quad (11)$$

where f_i' and f_j' are the Fermi functions for the i th and the j th levels, respectively, M_{ij}^2 is the transition momentum matrix element for each subband level pairs. The total gain function is the sum of g_{ij} over all allowed transitions and Lorentzian function is used to broaden the gain spectrum^[6]. In our model, a scattering life time of 0.8×10^{-13} s is used.

3 Results and Discussion

Here all calculations are for a typical 1.25Q barrier lattice matched to InP. The emission wavelength is defined as the peak material gain wavelength when the surface density $N_s = 1.5 \times 10^{16} \text{ m}^{-2}$. Temperature of 300K is adopted in all of our calculations.

Figure 2 shows the relations between well width and strain with different Ga compositions. Some experimental results have been compared with calculated ones, which agree with each other. For example, the well width of $\text{In}_{0.65}\text{Ga}_{0.34}\text{Al}_{0.01}\text{As}$ well material is 5.7nm in our calculation, which agrees very well with the experimental results $L_z = 5.4\text{nm}$. For the unstrained $\text{In}_{0.53}\text{Ga}_{0.47}\text{As}$ well material, a well width of 8.6nm has been reported^[6], while what we obtained is 9.0nm in the calculation. Again there is a good agreement. The relations between well width and Al composition with different Ga compositions are presented in Fig. 3. From the calculated results, when $0 \leq x \leq 0.17$ (Al composition) and $0 \leq y < 0.47$ (Ga composition), there is a compressive strain for the In_{1-x-y}

Ga_yAl_xAs system.

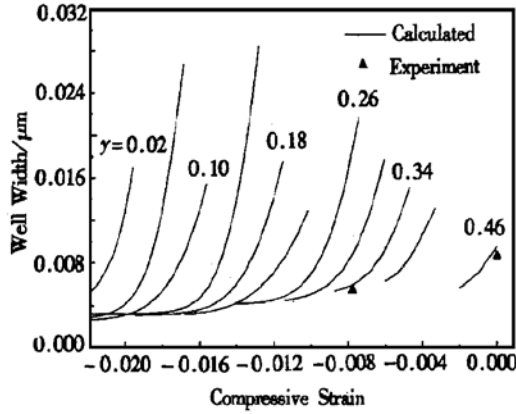


FIG. 2 Relations Between Well Width and Strain for Lasers

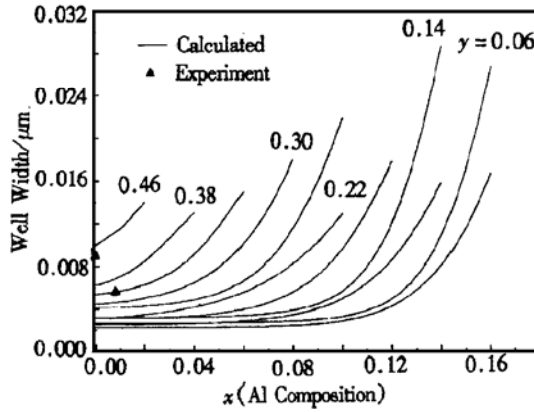


FIG. 3 Relations Between Well Width and Al Composition for In_{1-x-y}Ga_yAl_xAs Lasers

When $0.47 < y < 0.6$, there is a tensile strain, but x value is nearly zero, so the In_{1-x-y}Ga_yAl_xAs system changes into the In_{1-y}Ga_yAs ternary system. In this paper, we only study the case of compressive strain.

For the sake of convenience in the device design, we present the following empirical formulas:

Let well width L_z (in m) as a function of the compositional parameters x and y (for the quaternary In_{1-x-y}Ga_yAl_xAs compressive strain):

$$L_z(x, y) = \sum_{i,j} L_{ij} x^i y^j, \quad (12)$$

where $i = 4, 3, 2, 1, 0, j = 5, 4, 3, 2, 1, 0$.

The above formula does not err by more than 0.5nm compared with the numerical calculations.

Coefficients L_{ij} are list in Appendix.

For the quantum wells, the linear gain may be expressed as

$$g_L = a_N \ln(N/N_t) \quad (13)$$

where a_N is the characteristic gain; N_t is the transparency carrier density. Note that it has been pointed out by several authors^[6] that near threshold, the relation between the optical gain and the carrier density is a logarithmic one. Our calculations are based on a fixed surface density of $N_s = 1.5 \times 10^{16} \text{ m}^{-2}$. Figure 4 shows that there is a decrease in the characteristic gain with Al or Ga composition increasing and a larger characteristic gain can be ob-

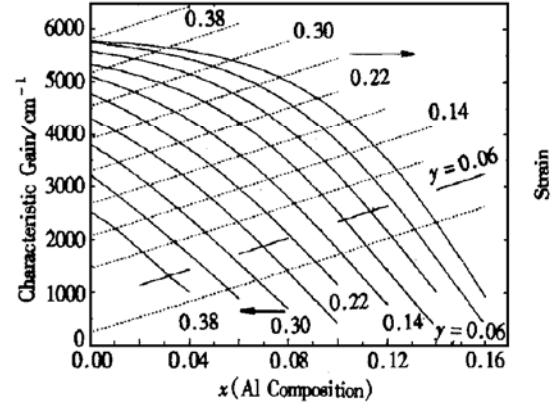


FIG. 4 Relations Between Characteristic Gain and Al Composition

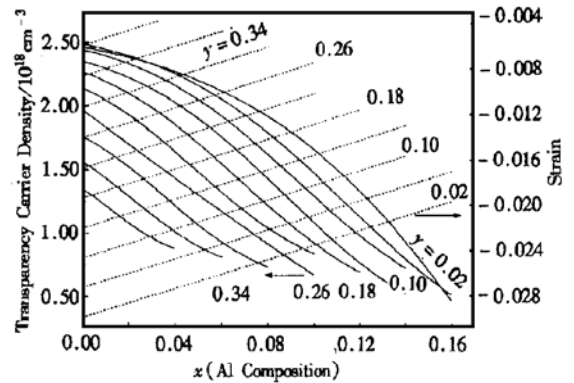


FIG. 5 Relations Between Transparency Carrier Density and Al Composition

tained due to the large compressive strain. For Al or Ga composition, the transparency carrier density has the same varying trend as the characteristic

gain, as shown in Fig. 5. Large characteristic gain and low transparency carrier density are known in favor of design of low threshold current, so the composition optimization must be done to obtain the suitable characteristic gain and transparency carrier density.

On the other hand, a high differential gain is necessary to the design of high modulation speed

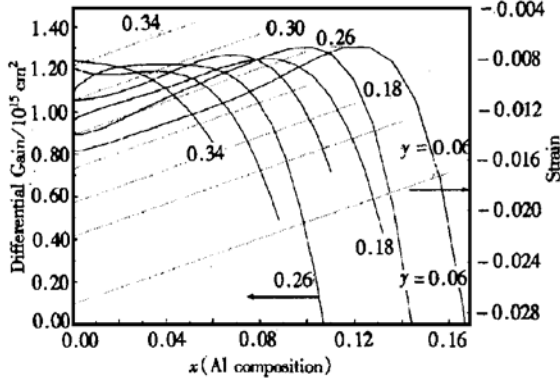


FIG. 6 Relation Between Differential Gain and Al Composition

lasers. The differential gain is the function of carrier density. In our calculations, a fixed surface carrier density has been considered. In Fig. 6, it is observed that the differential gain arrives at the maximal value when Al composition increasing; and with the Ga composition increasing, the position of differential gain peak moves to a smaller x value (Al composition). In practice, these results can be used as a FYI in the device design.

Some comparisons have been done between $\text{In}_{1-x-y}\text{Ga}_y\text{Al}_x\text{As}$ and $\text{In}_{1-x}\text{Ga}_x\text{As}_{1-y}\text{P}_y$ systems in characteristic gain and transparency carrier density. For the same strain and well width with InP barrier, higher characteristic gain can be found in $\text{In}_{1-x-y}\text{Ga}_y\text{Al}_x\text{As}$ system but higher transparency carrier densities in InP barrier, as shown in Table 2. But the difference in transparency carrier density can hardly affect the gain, so at the same injection, $\text{In}_{1-x-y}\text{Ga}_y\text{Al}_x\text{As}$ system has a higher gain.

Table 2 Characteristic Gain and Transparency Carrier Density in $\text{In}_{1-x-y}\text{Ga}_y\text{Al}_x\text{As}$ and $\text{In}_{1-x}\text{Ga}_x\text{As}_{1-y}\text{P}_y$ Systems

Material	x	y	Strain	Well Width /nm	Characteristic Gain/ cm^{-1}	Transparency Carrier Density/ 10^{17}cm^{-3}
$\text{In}_{1-x-y}\text{Ga}_y\text{Al}_x\text{As}$	0.05	0.3	-0.008	9.375	1539	8.79
$\text{In}_{1-x}\text{Ga}_x\text{As}_{1-y}\text{P}_y$	0.3	0.1	-0.008	9.375	1292	8.75
$\text{In}_{1-x-y}\text{Ga}_y\text{Al}_x\text{As}$	0.05	0.35	-0.0047	13.50	865	7.2
$\text{In}_{1-x}\text{Ga}_x\text{As}_{1-y}\text{P}_y$	0.374	0.05	-0.0047	13.50	736	6.96
$\text{In}_{1-x-y}\text{Ga}_y\text{Al}_x\text{As}$	0.05	0.25	-0.0115	7.00	1969	10.0
$\text{In}_{1-x}\text{Ga}_x\text{As}_{1-y}\text{P}_y$	0.275	0.05	-0.0115	7.00	1336	10.0
$\text{In}_{1-x-y}\text{Ga}_y\text{Al}_x\text{As}$	0.1	0.1	-0.0183	7.125	1982	9.27
$\text{In}_{1-x}\text{Ga}_x\text{As}_{1-y}\text{P}_y$	0.175	0.05	-0.0183	7.125	568	8.42

The empirical formulas for the characteristic gain a_n (in $1/\text{cm}$) and transparency carrier density N_t (in cm^{-3}) as functions of compositional parameters x and y are as follows:

$$a_n(x, y) = \sum_{i,j} a_{ij} x^i y^j, \quad (14)$$

$$N_t = \sum_{i,j} N_{ij} x^i y^j, \quad (15)$$

where $i = 4, 3, 2, 1, 0, j = 5, 4, 3, 2, 1, 0$. The error between numerical calculations and above formulas are both less than 10%. Coefficients a_{ij} and N_{ij} are listed in Appendix.

When we change the composition in the barrier

(which is kept lattice matched to InP), we find that as the barrier potential is away from $1.25Q$, the well width and optical gain (13) vary by the same factor approximately. A factor can be expressed as the function of well composition and barrier band gap:

$$F = (-12.8 + 754x - 143y - 3100x^2 + 4783y^2 - 9158xy) \left(\frac{1}{1.25} - \frac{1}{Q} \right) + 1 \quad (16)$$

where Q is the wavelength (μm) of the barrier material.

4 Conclusion

A simple and useful method is presented to analyze the band structure, in which, Harrison's model and anisotropic parabolic approximation are used in the calculation. To design the $\text{In}_{1-x-y}\text{Ga}_y\text{Al}_x\text{As}$ compressive strain quantum well, we discuss the relations between the well width and composition. The differential gain, transparency carrier density and the characteristic gain are also discussed.

Reference

[1] J. S. Osinski, Y. Zou, P. Grodzinski, A. Mathur and P. D. Dap-

kus, IEEE Photon. Technol. Lett., 1992, **4**: 10—13.

[2] P. J. A. Thijs, L. F. Tiemijer, J. J. M. Binsma and T. van Dongen, IEEE J. Quantum Electron., 1994, **30**: 477—499.

[3] C. E. Zah and R. Bhat, IEEE J. Quantum Electron., 1994, **30**: 511—523.

[4] M. Allovon and M. Quillec, Proc. Inst. Elect. Eng., 1992, **139**: 148—152.

[5] J. Minch, S. H. Park, T. Keating and S. L. Chuang, IEEE J. Quantum Electron., 1999, **35**: 771—782.

[6] T. - A. Ma and Z. - M., IEEE J. Quantum Electron., 1995, **31**: 29—34.

[7] E. Zielinski and F. Keppler, J. Quantum Electron., 1987, **QE-23**: 969—976.

[8] K. H. Hellwege, Ed., Landolt-Bornstein Numerical Data and Functional Relationships in Science and Technology, Berlin, Germany: Springer, 1982, new series, group III, 17a; groups III—V 22a, Berlin: Springer, 1986.

[9] Zhan-Ming Li and Michel Dion, IEEE J. Quantum Electron., 1993, **29**: 346—354.

Appendix A

Coefficients for Empirical Well Width Formulas(L_{ij})

	y^0	y^1	y^2	y^3	y^4	y^5
x^0	0.1824×10^{-8}	0.3089×10^{-9}	-0.3034×10^{-7}	0.1084×10^{-5}	-0.6117×10^{-5}	0.1043×10^{-4}
x^1	-0.6873×10^{-7}	-0.1039×10^{-5}	0.9952×10^{-4}	-0.1495×10^{-2}	0.7427×10^{-2}	-0.1165×10^{-1}
x^2	0.2712×10^{-5}	0.1011×10^{-3}	-0.5710×10^{-2}	0.7971×10^{-1}	-0.3858	0.5973
x^3	-0.2620×10^{-4}	-0.2092×10^{-2}	0.9377×10^{-1}	-0.1242×10^1	0.5888×10^1	-0.9022×10^1
x^4	0.7130×10^{-4}	0.1178×10^{-1}	-0.4568	0.5822×10^1	-0.2719×10^2	0.4140×10^2

Coefficients for Empirical Characteristic Gain Formulas(a_{ij})

	y^0	y^1	y^2	y^3	y^4	y^5
x^0	0.4980×10^4	0.4852×10^5	-0.8273×10^6	0.5652×10^7	-0.1779×10^8	0.2069×10^8
x^1	0.9707×10^5	-0.5988×10^7	0.9430×10^8	-0.6255×10^9	0.1842×10^{10}	-0.1982×10^{10}
x^2	-0.3367×10^7	0.2154×10^9	-0.3503×10^{10}	0.2353×10^{11}	-0.7019×10^{11}	0.7656×10^{11}
x^3	0.4137×10^8	-0.2841×10^{10}	0.4714×10^{11}	-0.3227×10^{12}	0.9786×10^{12}	-0.1083×10^{13}
x^4	-0.1805×10^9	0.1243×10^{11}	-0.2102×10^{12}	0.1461×10^{13}	-0.4477×10^{13}	0.4986×10^{13}

Coefficients for Empirical Transparency Carrier Density Formulas(N_{ij})

	y^0	y^1	y^2	y^3	y^4	y^5
x^0	0.2238×10^{19}	0.1304×10^{20}	-0.2099×10^{21}	0.1391×10^{22}	-0.4364×10^{22}	0.5057×10^{22}
x^1	0.9735×10^{19}	-0.5581×10^{21}	0.5831×10^{22}	-0.2454×10^{23}	0.3316×10^{23}	0.5025×10^{22}
x^2	-0.2156×10^{21}	0.4633×10^{22}	0.3432×10^{23}	-0.8520×10^{24}	0.4225×10^{25}	-0.6279×10^{25}
x^3	0.5768×10^{21}	0.2062×10^{23}	-0.1710×10^{25}	0.1916×10^{26}	-0.7817×10^{26}	0.1055×10^{27}
x^4	0.8553×10^{21}	-0.2814×10^{24}	0.1021×10^{26}	-0.1009×10^{27}	0.3951×10^{27}	-0.5183×10^{27}

1.55 μm $\text{In}_{1-x-y}\text{Ga}_y\text{Al}_x\text{As}$ 压缩应变量子阱激光器的近似阱宽和光增益公式*

张冶金 陈维友 蒋 恒 刘彩霞 刘式墉

(集成光电子学国家重点实验室吉林大学实验区, 长春 130023)

摘要: 应用 Harrison 模型和各向异性抛物带近似理论计算了 $\text{In}_{1-x-y}\text{Ga}_y\text{Al}_x\text{As}$ 压缩应变量子阱的能带结构. 为设计 $1.55\mu\text{m}$ 发射波长的激光器, 对可能组分范围内材料的阱宽、微分增益、透明载流子浓度做了系统分析, 得到一些有用的拟合公式.

关键词: $\text{In}_{1-x-y}\text{Ga}_y\text{Al}_x\text{As}$; 量子阱激光器; 线性增益; 微分增益

PACC: 4255P; 4260; 7340L; 7280

中图分类号: TN248.4

文献标识码: A

文章编号: 0253-4177(2001)01-0011-07

* 国家自然科学基金(69937019), 吉林省优秀青年科学基金(19990529-2) 和国家高技术(863) 研究和计划(863-307-15-31081) 资助项目.

张冶金 男, 1973 年出生, 博士, 主要从事激光器 CAD 研究.

2000-07-06 收到, 2000-09-17 定稿

©2001 中国电子学会